Vulnerability analysis of RC buildings with wide beams located in moderate seismicity regions

F. López-Almansa [a,*], D. Domínguez [b], A. Benavent-Climent [c]

[a] Technical University of Catalonia, Architecture Structures Department, Avda. Diagonal 649, 08028 Barcelona, Spain
[b] International University of Catalonia, Architecture Department, Immaculada 22, 08017 Barcelona, Spain
[c] University of Granada, Department of Structural Mechanics, Edificio Politécnico, 18071 Granada, Spain

Keywords:
Seismic vulnerability
Concrete buildings
Wide beams
Push-over analysis
Spain

A B S T R A C T

A significant number of short-to-mid height RC buildings with wide beams have been constructed in areas of moderate seismicity of Spain, mainly for housing and administrative use. The buildings have a framed structure with one-way slabs; the wide beams constitute the distinctive characteristic, their depth being equal to that of the rest of the slab, thus providing a flat lower surface, convenient for construction and the layout of facilities. Seismic behavior in the direction of the wide beams appears to be deficient because of: (i) low lateral strength, mainly because of the small effective depth of the beams, (ii) inherent low ductility of the wide beams, generated by high amount of reinforcement, (iii) the big strut compressive forces developed inside the column-beam connections due to the low height of the beams, and (iv) the fact that the wide beams are wider than the columns, meaning that the contribution of the outer zones to the resistance of the beam-column joints is unreliable because there is no torsion reinforcement. In the orthogonal direction, the behavior is worse since the only members of the slabs that contribute to the lateral resistance are the joists and the façade beams. Moreover, these buildings were designed with codes that did not include ductility requirements and required only a low lateral resistance; indeed, in many cases, seismic action was not considered at all. Consequently, the seismic capacity of these structures is not reliable. The objective of this research is to assess numerically this capability, whereas further research will aim to propose retrofit strategies. The research approach consists of: (i) selecting a number of 3-story and 6-story buildings that represent the vast majority of the existing ones and (ii) evaluating their vulnerability through three types of analyses, namely: code-type, push-over and nonlinear dynamic analysis. Given the low lateral resistance of the main frames, the cooperation of the masonry infill walls is accounted for; for each representative building, three wall densities are considered. The results of the analyses show that the buildings in question exhibit inadequate seismic behavior in most of the examined situations. In general, the relative performance is less deficient for Target Drift CP (Collapse Prevention) than for IO (Immediate Occupancy). Since these buildings are selected to be representative of the vast majority of buildings with wide beams that were constructed in Spain without accounting for any seismic consideration, our conclusions can be extrapolated to a broader scenario.

1. Introduction

For the purpose of this study, Spain is divided into three seismic zones in terms of the design ground acceleration (a_g): low or no seismicity ($a_g < 0.08$ g), moderate seismicity ($0.08\ \text{g} \leqslant a_g < 0.16$ g) and medium (or mid) seismicity ($0.16\ \text{g} \leqslant a_g$); a significant number of RC buildings with wide beams are located in areas of moderate and medium seismicity. Most of the buildings are intended for use as a dwelling, though administrative use is also common. The buildings have a concrete framed structure with one-way slabs as the primary system. The wide beams constitute the distinctive characteristic, their width being greater than that of the supporting columns and their depth being equal to that of the rest of the slab, thus providing for a flat lower surface which facilitates construction of the slabs and layout of the facilities. Fig. 1 displays a sketch of a one-way slab with wide beams.

This type of floor is also common in other countries in Europe, such as France and Italy. Wide-beam technology is furthermore used in Australia and the US and Canada, where it is also known as banded-floor or slab-band system. In the latter countries, wide beams are utilized for car park buildings, with span-lengths that are significantly longer than those considered in the European buildings with wide beams. In Australia, meanwhile, the depth of the band beam is likely to be at least double that of the slab. In contrast to Australia, the US and Canada, in Mediterranean countries

* Corresponding author. Tel.: +34 93 4016316/606807733; fax: +34 93 4016096.
E-mail address: francesc.lopez-almansa@upc.edu (F. López-Almansa).

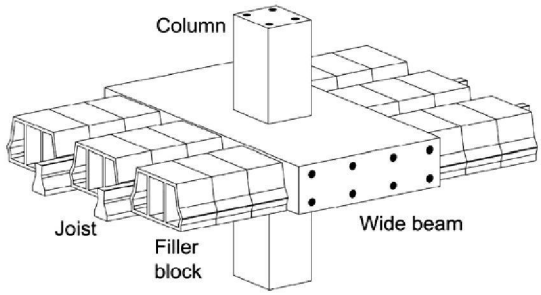

Fig. 1. One-way slab with wide beams.

the amount of reinforcement has to be high (commonly ranging between 2% and 6%), to compensate for insufficient effective depth.

The seismic behavior of buildings with wide beams could be deficient and calls for investigation. In the direction of the wide beams, the following weaknesses can be presumed:

- The lateral strength and stiffness of the building are low, mainly because the effective depth of the beams is small (as compared to that of conventional beams).
- The ductility of the wide beams is low since the amount of reinforcement is high.
- The strut compressive forces developed inside the column-beam connections are considerable, due to the low height of the beams.
- Since the beams are wider than the columns, a relevant part of the longitudinal reinforcement of the beams lies beyond the vertical projection of the columns (Fig. 1). Hence, the contribution of such outer zones of the beams to the bending resistance of the beam-column connections is unreliable, as the beams have no torsion reinforcement.

In the orthogonal direction, the lateral seismic behavior might be even worse, since the only members of the slabs that contribute to the lateral resistance of the buildings are the joists and the façade beams.

Furthermore, before 1994 these buildings were designed with codes that did not include ductility demands and that required only a low lateral resistance. In regions with moderate seismicity, seismic action was often not taken into account whatsoever. All these considerations would indicate that the seismic capacity of these structures is not reliable. The objective of our research is to numerically assess the seismic capability of wide-beam buildings situated in moderate seismicity areas of Spain and constructed mainly prior to 1994. The research approach consists of: (i) a study of the main features of these buildings and selection of a number of representative edifices, and (ii) analysis of the vulnerability of the selected buildings.

A relevant part of this study consists of investigating the hysteretic behavior of the beam-column connections; several researchers have experimentally analyzed the seismic performance of connections between wide beams and columns. Some studies refer to the US and Canada [16,29,14,18,19,31] while other works correspond to Australia [34,33,15]; most conclude that the seismic capacity of the tested connections is limited, and some researchers propose design criteria. Since the conditions of the wide-beam slabs in these countries differ significantly from those in Spain, the results cannot be applied directly to this study. In view of the significant number of potentially vulnerable wide-beam buildings in Spain and that there is a lack of reliable information, a research project aiming to assess the seismic capacity of potentially vulnerable buildings located in seismic prone areas of Spain and to propose retrofit strategies was launched a few years ago. The present contribution is part of this broader research effort. Two construction typologies were considered: waffle slabs and wide-beam slabs. Regarding buildings with wide beams, previous research consisted mainly of cyclic testing on connections between wide beams and columns [3,4] and of numerically investigating the seismic vulnerability of buildings with wide beams located in regions of Spain with medium seismicity [5]. Conversely, this work focuses on buildings located in regions of Spain with moderate seismicity; the obtained experimental results are used in both numerical studies. Further research will aim to propose retrofit strategies for RC buildings with wide beams situated in Spain. This research might be also useful for similar constructions located in nearby countries, as France and Italy.

2. Buildings studied

Six prototype buildings were chosen to represent the vast majority of the edifices with wide beams located in moderate seismicity areas of Spain; all have four bays in both directions, and two of the buildings have three floors while the other four have six floors. They are depicted in Fig. 2 while Fig. 3 displays a plan view of a slab and two cross-sections of a wide beam and of secondary beams, respectively. Figs. 2 and 3 show that the buildings considered are regular and quite symmetric; hence, no relevant twisting effects are expected. Fig. 3a shows that in the x direction every one-way slab contains five wide beams while in the y direction there are two (outer) façade beams and three (inner) joists that are coplanar with columns. Fig. 3b and c shows that the wide beams are wider than the columns, whereas the width of the façade beams is equal to the one of the columns. Fig. 3b and c also shows that the joists are semi-prefabricated, being composed of a lower "sole" and a "truss-type" naked reinforcement; since pre-stressed, pre-fabricated beams are also commonly employed as joists, they have were likewise considered in our analyses. The top concrete layer is 4 cm thick and is not reinforced. Fig. 3c shows the top splice bars that guarantee the continuity of the joists, though merely placed over them.

Table 1 describes the main characteristics of the considered buildings; in the notation 3 – 5 – ■, "3" refers to the number of floors, "5" corresponds to the span-length in both directions and "■" means that the columns have a square cross-section. The fundamental periods correspond to the direction of the wide beams and to the orthogonal one, respectively, and are indicated as x and y in Figs. 2 and 3. The periods were determined from the numerical models of the buildings described in Section 4, to be considered for the push-over and dynamic analyses (Sections 5 and 6, respectively). The last column contains the total weight of the buildings; the influence of the walls was neglected [7].

Since the selected buildings possess only low lateral resistance, the cooperation of the infill walls cannot be neglected. In this study, however, only the contribution of walls made with "Group 2" brick units [10] 12 cm thick was accounted for. The walls whose contribution is neglected are either the ones structurally detached from the main frame or those made of 4 cm thin bricks (Group 3 or 4 brick units). The walls of the first type are not considered because they are not affected by the drift motion of the main structure; the walls of the second type are neglected because their behavior is too brittle to allow the deformations required by the plastic strut-and-tie behavior [21]. For each of the six representative buildings three wall densities were considered: no walls, low density and high density. The first and second cases correspond to commercial buildings with light claddings, while the third case corresponds to houses. Fig. 4 depicts typical layouts of the walls for the second and third cases. Since the infill walls are placed symmetrically in both directions, the horizontal behavior will be also symmetric.

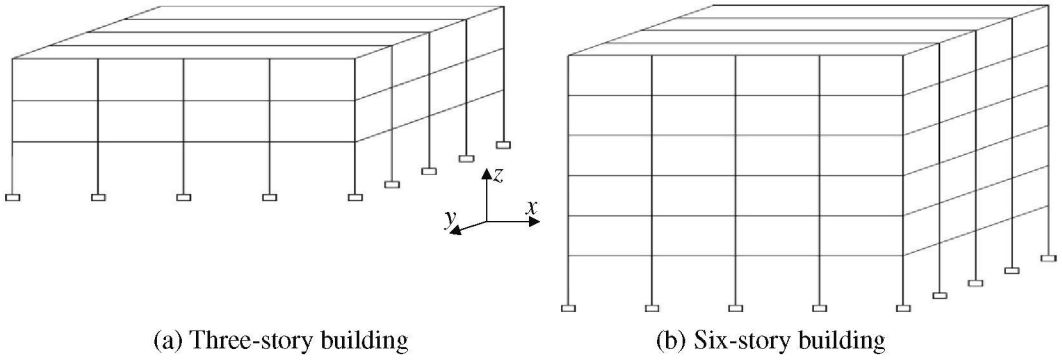

Fig. 2. Selected representative buildings.

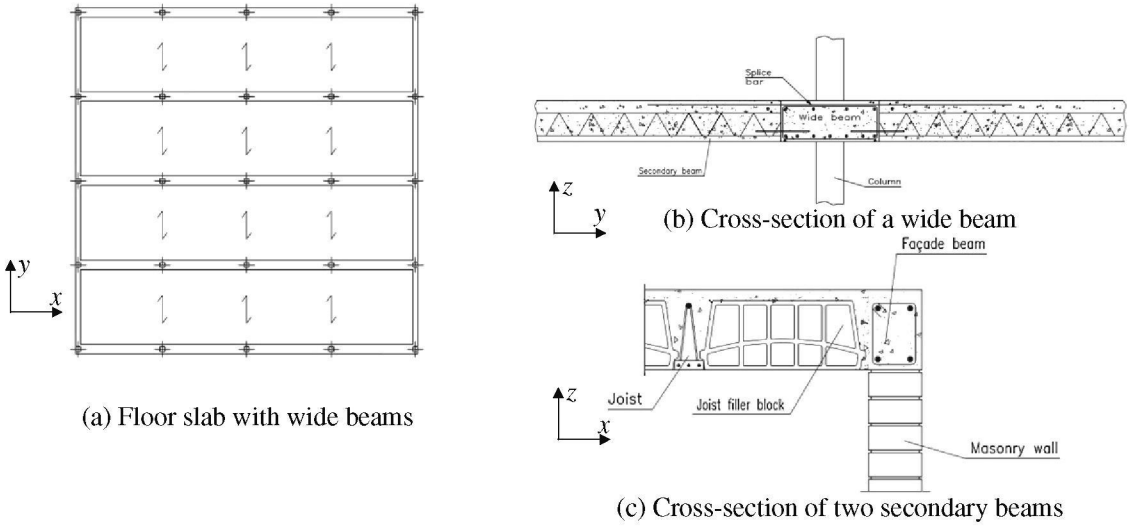

Fig. 3. Building slab with wide beams.

Table 1
Representative buildings.

Building	Stories/height (m)	Span-lengths of the beams (m)	Plan size (m)	Wide beams (cm)	First floor columns (cm)	Top floor columns (cm)	Fundamental periods w/o walls (x/y) (s)	Weight (kN)
3–5 – ■	3/10	5 × 5	20 × 20	25 × 60	40 × 40	30 × 30	0.585/1.037	9770
3–5.5 – ■	3/10	5.50 × 5.50	22 × 22	29 × 75	40 × 40	30 × 30	0.783/1.309	10,825
6–5 – ■	6/19	5 × 5	20 × 20	25 × 60	50 × 50	30 × 30	1.333/2.630	20,310
6–5.5 – ■	6/19	5.50 × 5.50	22 × 22	29 × 75	50 × 50	30 × 30	1.364/2.989	25,640
6–5 – ■	6/19	5 × 5	20 × 20	25 × 60	60 × 50	40 × 30	1.206/2.480	20,875
6–5.5 – ■	6/19	5.50 × 5.50	22 × 22	29 × 90	60 × 50	40 × 30	1.241/2.836	26,115

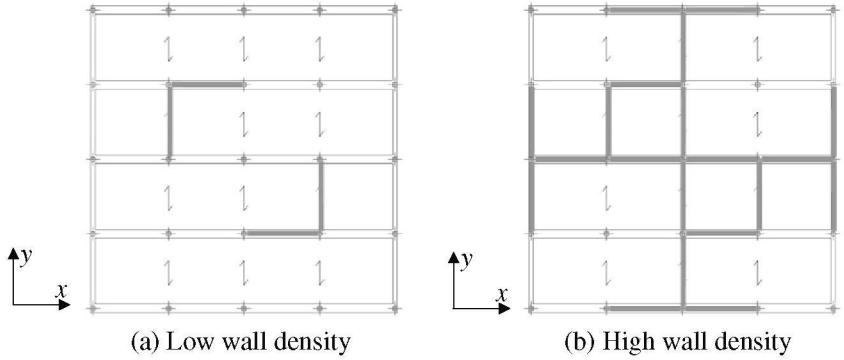

Fig. 4. Layout of the infill walls in the considered buildings.

All these walls are assumed to be continuous down to the foundation.

The characteristic value of the concrete compressive strength is 17.5 MPa. The steel type is AEH 400 S [8]; its yielding point and ultimate stress are 410 MPa and 530 MPa, respectively, and the ultimate strain is 14%. In the infill walls, the characteristic values of the brick and mortar strengths are 12 and 8 MPa, respectively; the characteristic strength is $f_k = Kf_b^{0.70}f_m^{0.30} = 0.45 \times 12^{0.70} \times 8^{0.30} = 4.781$ MPa [10] and the secant deformation moduli [21] are $E = 500f_k = 2391$ MPa (longitudinal) and $G = 0.4E = 956$ Mpa (transverse). The value of coefficient K has been chosen according to the brick unit type (clay, group 2), the mortar (general purpose) and the presence of longitudinal joints.

3. Code-type analyses

The seismic performance of the selected buildings is assessed according to the current Spanish [25] and European [11] seismic design codes. In both cases the analyses consisted of determining static equivalent forces in both horizontal directions; then, the corresponding damage level was estimated from the capacity curves derived from the push-over analyses described in Section 5. The static forces were obtained from the response spectra for 5% damping and design seismic accelerations 0.08 g and 0.11 g; according to Spanish regulations, these accelerations correspond to stiff soil and to a 500 year return period. For each building, the four major soil types included in both codes have been considered. The Eurocode denotes them as soil A (rock, $v_{s,30} > 800$ m/s where $v_{s,30}$ is the shear wave velocity averaged over the top 30 m of soil), B (stiff soil, $360 < v_{s,30} < 800$ m/s), C (soft soil, $180 < v_{s,30} < 360$ m/s) and D (very soft soil, $v_{s,30} < 180$ m/s). For these soil types, the right-hand edge of the plateau corresponds to periods ranging from 0.4 s to 0.8 s in Spanish regulations [25] and from 0.25 s to 0.30 s in European regulations [11]. The response reduction factor is assumed as $\mu = 2$ in the Spanish code and as $q = 1.5$ in the Eurocode, regardless of the wall density. The fundamental periods of the buildings with infill walls were determined by correcting those of the buildings without walls (see Table 1) with the empirical expressions proposed by Eurocode 6 [10]. The results obtained show that the consideration of the walls significantly increases the stiffness of the buildings [7]. Table 1 shows that the fundamental periods of the buildings without walls lie in the descending branch of the design spectra; conversely, a number of the periods of the buildings with walls lay inside the plateau. Therefore, the stiffening effect of the walls significantly increases the seismic equivalent forces. No accidental eccentricity is considered in the derivation of the equivalent seismic forces.

Comparison between the seismic forces prescribed by Spanish and European regulations [7] shows them to be similar. Table 2 displays the most demanding base shear coefficients. Results from Table 2 show that the base shear coefficient increases as does the wall density (except for soil D and 3 – 5 – ■ building); it ranges between 0.01 for the transverse direction (y) of building 6 – 5.5 – ■ without walls (soil A and design acceleration 0.08 g) and 0.249 for the longitudinal direction (x) of building 3 – 5 – ■ with low wall density (soil D and design acceleration 0.11 g).

Table 2
Base-shear coefficients (V/W) according the Spanish and European regulations.

Building	Direction	Wall density	Design acceleration 0.08 g				Design acceleration 0.11 g			
			Soil A	Soil B	Soil C	Soil D	Soil A	Soil B	Soil C	Soil D
3 – 5 – ■	Wide beams (x)	None	0.052	0.089	0.123	0.153	0.072	0.122	0.168	0.211
		Low	0.077	0.114	0.127	0.183	0.115	0.156	0.173	0.249
		High	0.077	0.120	0.134	0.161	0.122	0.164	0.183	0.219
	Transversal (y)	None	0.029	0.050	0.076	0.118	0.040	0.068	0.104	0.163
		Low	0.079	0.106	0.123	0.170	0.107	0.145	0.168	0.232
		High	0.089	0.120	0.134	0.161	0.122	0.164	0.183	0.219
3 – 5.5 – ■	Wide beams (x)	None	0.039	0.066	0.100	0.153	0.053	0.091	0.138	0.208
		Low	0.077	0.100	0.123	0.157	0.105	0.137	0.169	0.214
		High	0.089	0.121	0.134	0.161	0.122	0.165	0.183	0.219
	Transversal (y)	None	0.023	0.039	0.060	0.093	0.032	0.054	0.082	0.127
		Low	0.077	0.100	0.123	0.153	0.105	0.137	0.169	0.208
		High	0.089	0.121	0.134	0.161	0.122	0.165	0.183	0.219
6 – 5 – ■	Wide beams (x)	None	0.022	0.037	0.056	0.087	0.030	0.051	0.077	0.118
		Low	0.069	0.094	0.116	0.145	0.100	0.129	0.159	0.197
		High	0.089	0.120	0.134	0.161	0.122	0.164	0.183	0.219
	Transversal (y)	None	0.013	0.019	0.028	0.045	0.017	0.026	0.039	0.061
		Low	0.069	0.094	0.116	0.145	0.100	0.129	0.159	0.197
		High	0.089	0.120	0.134	0.161	0.122	0.164	0.183	0.219
6 – 5.5 – ■	Wide beams (x)	None	0.021	0.036	0.054	0.085	0.029	0.049	0.074	0.116
		Low	0.065	0.094	0.116	0.145	0.089	0.129	0.159	0.197
		High	0.089	0.120	0.134	0.161	0.122	0.164	0.183	0.219
	Transversal (y)	None	0.010	0.016	0.025	0.039	0.013	0.023	0.034	0.053
		Low	0.065	0.094	0.116	0.145	0.089	0.129	0.159	0.197
		High	0.089	0.120	0.134	0.161	0.122	0.164	0.183	0.219
6 – 5 – ■	Wide beams (x)	None	0.024	0.040	0.061	0.096	0.033	0.055	0.084	0.130
		Low	0.072	0.094	0.116	0.145	0.100	0.129	0.159	0.199
		High	0.089	0.121	0.134	0.161	0.122	0.165	0.183	0.219
	Transversal (y)	None	0.012	0.020	0.030	0.047	0.016	0.027	0.041	0.063
		Low	0.072	0.094	0.116	0.145	0.100	0.129	0.159	0.199
		High	0.089	0.121	0.134	0.161	0.122	0.165	0.183	0.219
6 – 5.5 – ■	Wide beams (x)	None	0.023	0.039	0.059	0.093	0.032	0.054	0.082	0.127
		Low	0.065	0.094	0.116	0.143	0.090	0.129	0.159	0.197
		High	0.089	0.120	0.134	0.161	0.122	0.164	0.183	0.219
	Transversal (y)	None	0.012	0.018	0.027	0.041	0.017	0.025	0.037	0.056
		Low	0.065	0.094	0.116	0.143	0.090	0.129	0.159	0.197
		High	0.089	0.120	0.134	0.161	0.122	0.164	0.183	0.219

4. Numerical modeling of the structural behavior

The nonlinear static and dynamic structural behavior of the buildings in each direction is described with 2D finite element models. Beams and columns were modeled with frame elements and the infill walls were modeled with compression-only bars joining adjacent floors. The diaphragm effect of the floor slabs is accounted for by rigid fictitious pin-ended bars connecting the outer nodes of the frames. Since the top concrete layer is not reinforced, the cooperation of any effective width of the slab with the beams and joists is not accounted for. The connections between the columns and the wide beams (x direction) and between the columns and the façade beams (y direction) were modeled as rigid since the reinforcement is assumed to be satisfactorily anchored [7]. Conversely, the connections between the columns and the joists (y direction) were modeled as rigid for negative bending moments yet are considered as ordinary hinges for positive bending moments since Fig. 3b shows that the lower reinforcement bars are not adequately anchored.

The behavior of concrete and steel is described by classical uniaxial constitutive laws; the stress–strain diagram for steel is bilinear, with strain hardening while the one of concrete is a parabola-rectangle model where the tension strength is neglected [9].

In both the x and y frames, the nonlinear behavior is concentrated in plastic hinges located at both ends of each member; the length of each plastic hinge is estimated as half of the depth of the cross-section of the member [32]. In the six considered buildings it was thoroughly checked that positive moment hinges did not form along the span of the beam [7]. The hysteretic behavior of the plastic hinges of the columns, of the wide beams (x direction, see Figs. 2 and 3) and of the façade beams and the joists (y direction) is described by trilinear laws. Such laws are characterized by the cracking, yielding and failure moments and curvatures; these moments were determined according to [1] and the obtained results were compared to those provided by the program Response 2000 [6], the agreement proving satisfactory. The cracking curvature was determined from the initial sectional stiffness, calculated

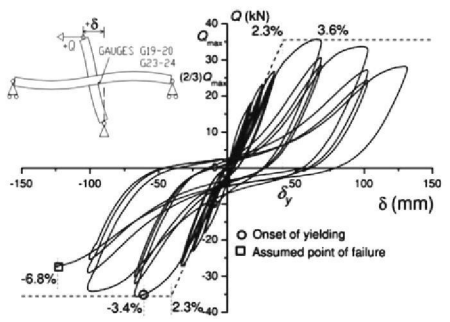

(a) Experimental loops [Benavent et al. 2010]

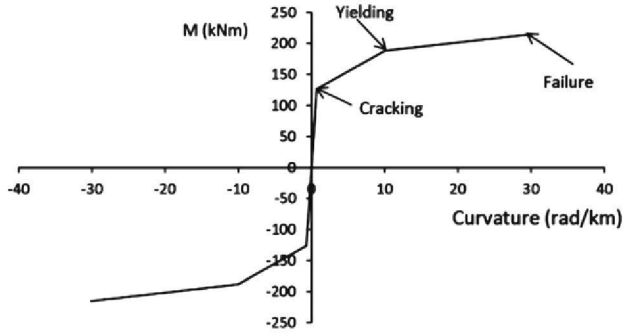

(b) Back-bone envelope for a column

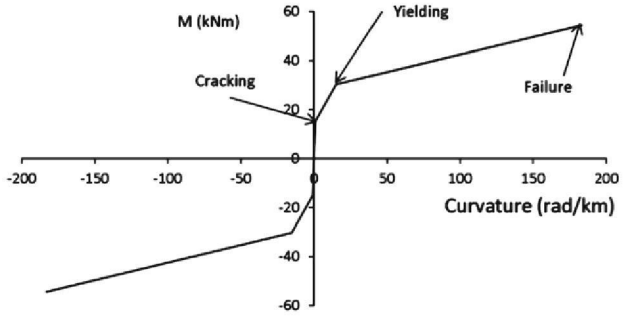

(c) Back-bone envelope for an end wide beam

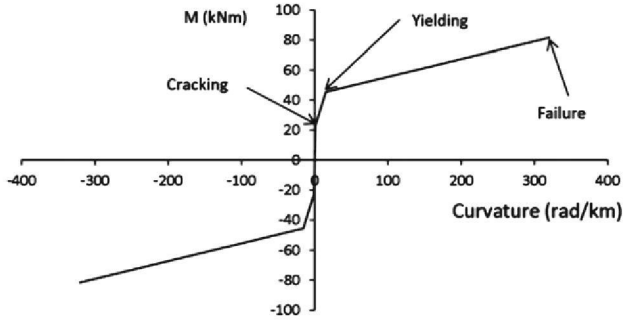

(d) Back-bone envelope for an inner wide beam

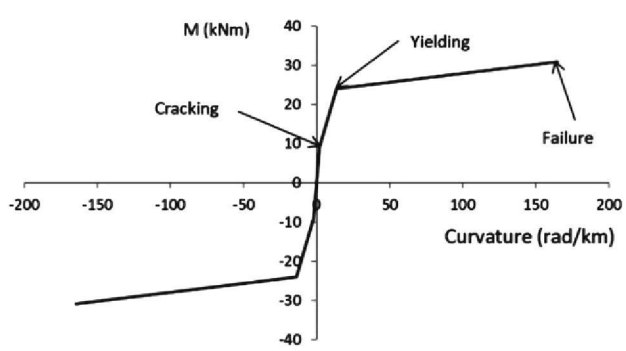

(e) Back-bone envelope for a façade beam

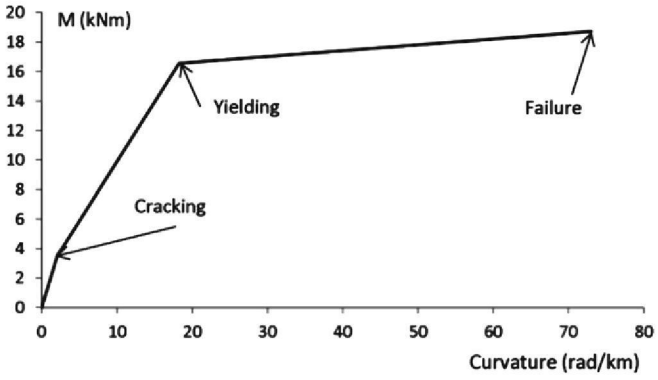

(f) Back-bone envelope for a joist

Fig. 5. Hysteretic model of a connection between a column and beams and joists.

by classical linear analyses, accounting for the contribution of the reinforcement bars. The yielding curvature was determined as suggested in [35]. The ultimate curvature of the wide beams and of the columns was determined according to the experimental results described in [3,4]; these authors suggest estimating such curvature by multiplying the yielding curvature by a ductility factor equal to 12 for the wide beams belonging to outer connections, to 21 for the wide beams belonging to inner connections, and to 3 for the columns. The ductility factor of the façade beams (y direction) is assumed to be equal to the one of the end wide beams. Given the lack of experimental results about the joists, their ultimate ductility curvature was conservatively estimated as 4; remarkably, since the contribution of the joists to the transverse lateral resistance is rather low, it is expected that the overall behavior of the buildings in transverse direction (y) is not very sensitive to this parameter. In the columns, the interaction with the compressive axial force is taken into account [32]. Fig. 5a shows experimental hysteresis loops [4] of a connection between a wide beam and a column. In turn, Fig. 5b–d shows back-bone envelopes adopted for the numerical modeling of a column and an outer and an inner wide beam, respectively. Fig. 5e and f display such constitutive laws for a façade beam and a joist, respectively. In the experiments described in [4] that were used in this study for modeling and calibrating the wide beam-column connections, no sign of joint shear failure was observed. Accordingly, the analytical model used here does not consider the possibility of joint shear failure. It is worth noting that the wide-beam column sub-assemblies tested by [3,4] and used in this study for calibrating the wide-beams of the models (Fig. 5) exhibited a strong column-weak beam mechanism. However, the collapse mechanism of the frames investigated in this study did not follow a strong column-weak beam pattern. Therefore, the local drifts of the tested wide-beam column subassemblies cannot be compared with the global drift of the building presented later in Section 5 (Fig. 13). The modeling of the wide-beams took into account the tendency observed during the tests of the inner bars to yield first in the negative moment region.

The hysteretic behavior of the masonry infill walls is represented by Bouc–Wen models [2]. Such models are characterized by two major parameters, i.e. the resistance and the initial stiffness. The resistance is obtained from tie-and-strut models, wherein two major failure modes are considered: diagonal strut compression and horizontal sliding along a course. In all the analyzed cases, the resistance for the first failure mode was significantly smaller. The possible "short column" effects [22] were not held to be relevant since the length of the columns that are not in contact with the diagonal struts is rather small [7]: for walls that are 3 m high and 5 m long it is 0.68 m, for walls that are 3 m high and 5.5 m long it is 0.72 m, for walls that are 4 m high and 5 m long it is 0.76 m, and for walls that are 4 m high and 5.5 m long it is 0.80 m. These values were obtained as suggested in [28]. The parameters for the tie-and-strut models were estimated as indicated by the Eurocode 6 [10]. As suggested in [24], the initial stiffness is estimated as two times the ratio between the ultimate resistance and displacement. The post-peak behavior is modeled as non-existent.

The finite element models of the frames and of the infill walls were jointly implemented in code IDARC-2D version 7.0 [32]; the hysteretic behavior of the plastic hinges of beams, columns and joists is modeled as discussed previously (Fig. 5). Furthermore, hysteretic curves based on sectional fiber models (derived from the aforementioned material constitutive laws) were also implemented in that code. Since the agreement between both types of analyses is satisfactory [7], for the sake of simplicity only calculations based on the hysteretic curves shown in Fig. 5 are considered in what follows.

Fig. 6 shows, for a given seismic input, the obtained hysteresis loops of a first floor column and a first floor end wide beam of building 3 – 5 – ■.

Plots from Fig. 6 show a regular hysteretic behavior. Comparison between Figs. 5 and 6 shows that the simulated loops match both the experimental loops and the theoretical back-bone envelopes.

5. Push-over analyses

Two-dimensional push-over analyses were carried out on the six buildings described in Table 1; for each building and each horizontal direction, the three aforementioned wall densities were considered. Since the behavior of the infill walls is described with dynamic models, the capacity curves were not obtained by classical static nonlinear analyses but with incremental nonlinear dynamic analyses using a given ground motion record scaled with different factors. The considered input is the NS component of the Tolmezzo-Diga Ambiesta ground motion record of the Friuli earthquake (06/05/1976) [12]. The results obtained with that register are compared with those calculated with other accelerograms belonging to the same data base; agreement is satisfactory. Moreover, for the buildings without walls, conventional incremental static analyses were carried out; no relevant differences were seen among them. Given the high lateral flexibility of the considered buildings, second-order analyses were performed; in most of the cases the differences with the first-order analyses were small. In the dynamic analyses, the time step is 0.01 s and the damping is described by a 5% Rayleigh model. Time integration was done using the Newmark-β method [26].

Figs. 7–12 show the capacity curves of the six considered buildings, respectively. Each Figure contains two sets of curves, the left

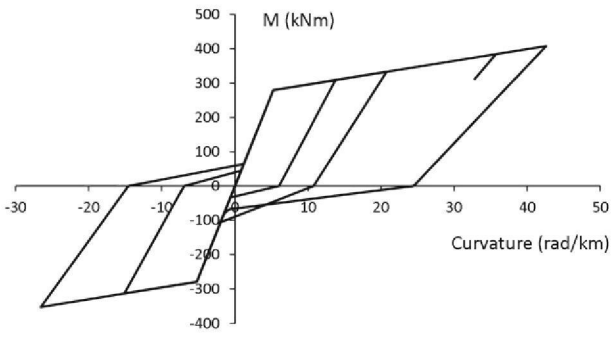

(a) Numerical hysteresis loops of a column

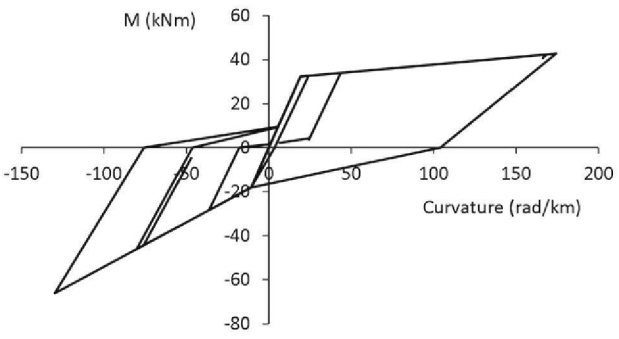

(b) Numerical hysteresis loops of an end wide beam

Fig. 6. Output hysteresis loops of members of the main frames (x direction).

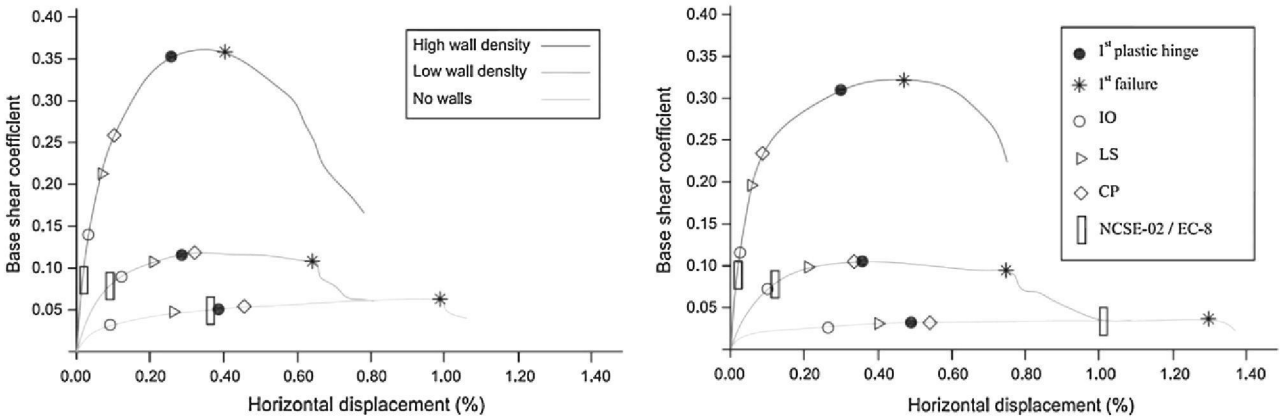

(a) Direction of the wide beams (x) (b) Transversal direction (y)

Fig. 7. Capacity curves, Target Drifts and onset of the plastic hinges of building 3 – 5 – ■ for soil A and design acceleration 0.08 g.

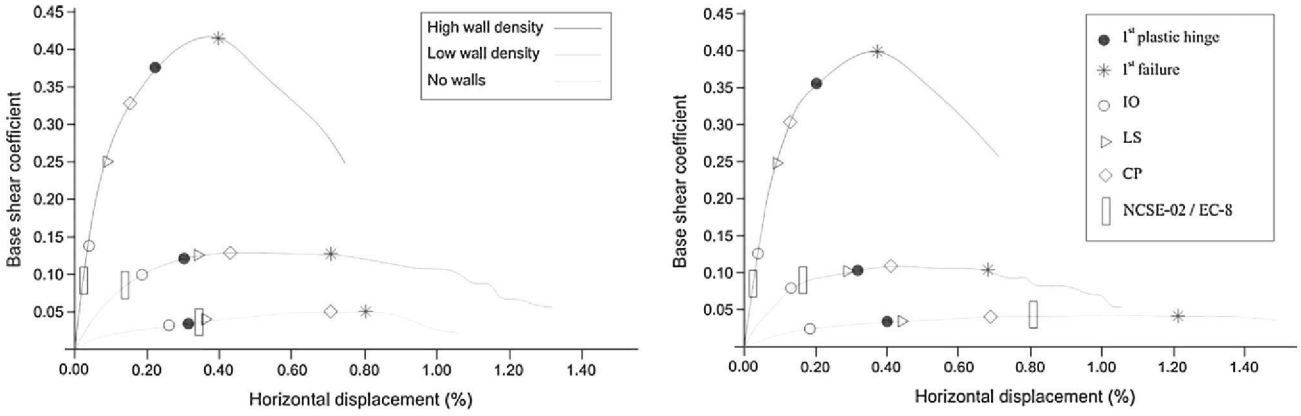

(a) Direction of the wide beams (x) (b) Transversal direction (y)

Fig. 8. Capacity curves, Target Drifts and onset of the plastic hinges of building 3 – 5.5 – ■ for soil A and design acceleration 0.08 g.

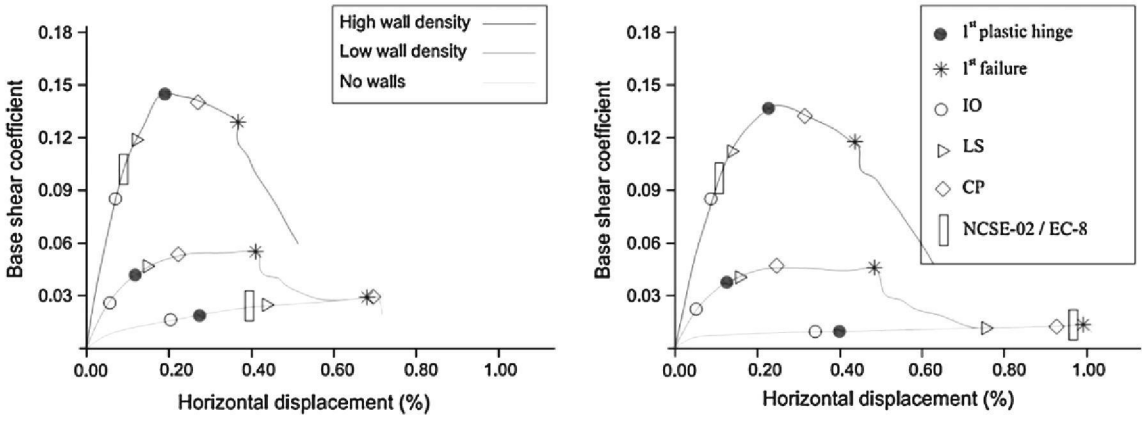

(a) Direction of the wide beams (x) (b) Transversal direction (y)

Fig. 9. Capacity curves, Target Drifts and onset of the plastic hinges of building 6 – 5 – ■ for soil A and design acceleration 0.08 g.

one corresponding to the direction of the wide beams (x), the right one corresponding to the transverse direction (y). Each set is composed of three curves that are associated with the case without walls, with low wall density and with high wall density, respectively. For each capacity curve, the performance points corresponding to the less demanding situation (soil A and design acceleration 0.08 g) are also represented. The Target Drifts (performance points) were determined, for each performance objective (IO "Immediate Occupancy", LS "Life Safety" and CP "Collapse Prevention") according to [13] by means of an iterative procedure, aiming to obtain the intersection between the capacity curve and the demanding spectrum that corresponds to the damping

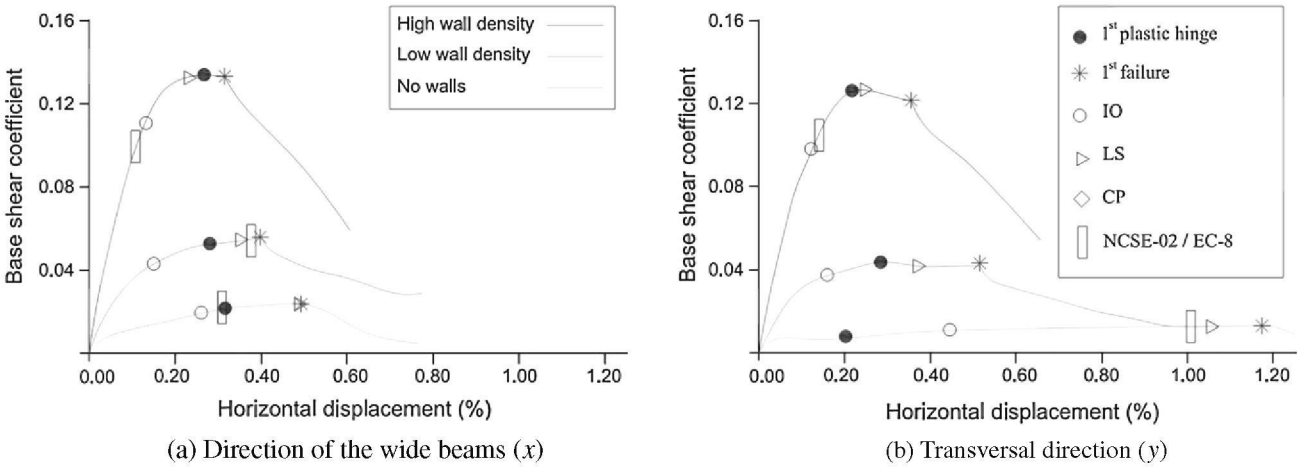

(a) Direction of the wide beams (x) (b) Transversal direction (y)

Fig. 10. Capacity curves, Target Drifts and onset of the plastic hinges of building 6 – 5.5 – ■ for soil A and design acceleration 0.08 g.

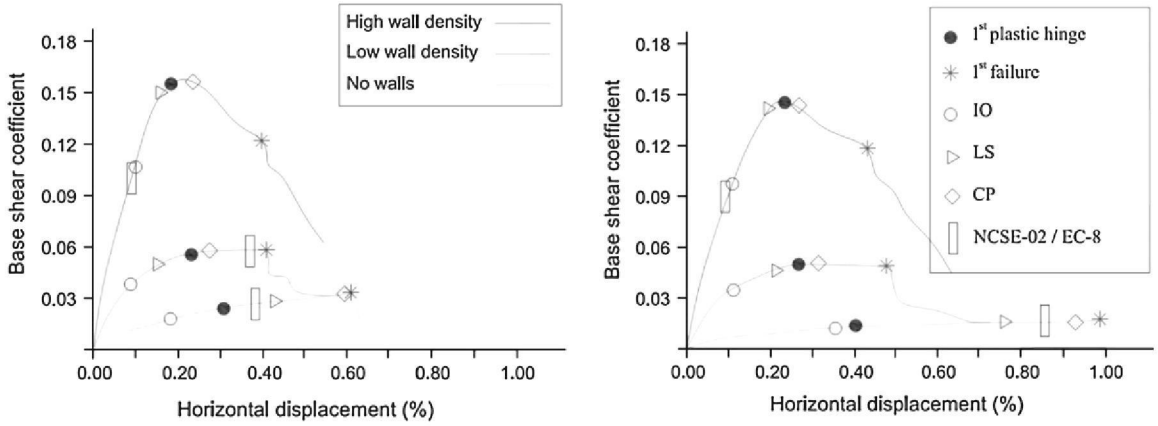

(a) Direction of the wide beams (x) (b) Transversal direction (y)

Fig. 11. Capacity curves, Target Drifts and onset of the plastic hinges of building 6 – 5 – ■ for soil A and design acceleration 0.08 g.

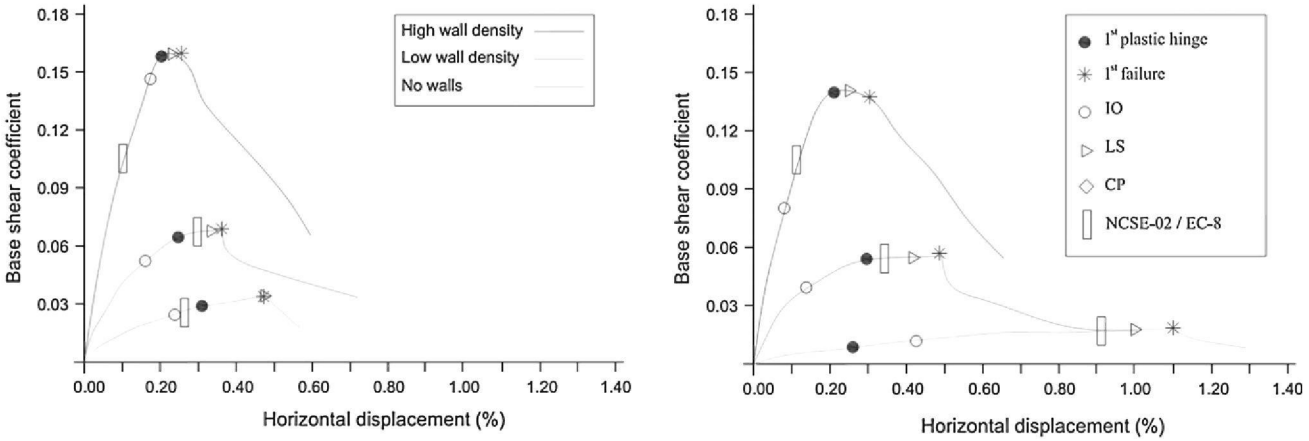

(a) Direction of the wide beams (x) (b) Transversal direction (y)

Fig. 12. Capacity curves, Target Drifts and onset of the plastic hinges of building 6 – 5.5 – ■ for soil A and design acceleration 0.08 g.

equivalent to the achieved damage. Because the use of the buildings is mainly of normal importance, these performance objectives are assigned to return periods of 100, 500 and 1000 years, respectively. For 500 years the design spectrum from the Spanish code [25] is adopted; for 100 and 1000 years that spectrum is modified according to the empirical expression suggested in that code. The performance points for IO, LS and CP are symbolised as "○", "▷" and "◇", respectively. In some capacity curves point "◇" is not present because the iterative procedure did not converge; this means that CP corresponds to collapse.

The points "□" indicate the design base shear coefficient prescribed by the most demanding design code, of the Spanish and the European. In certain capacity curves corresponding to low wall density, point "□" is not present because the equivalent forces prescribed by the codes are too high. Points "●" and "∗" stand for the formation of the first plastic hinge and for the first failure, respectively.

Plots from Figs. 7–12 reveal that the infill walls increase the seismic strength in both directions to a significant extent. Comparison between the left (a) and right (b) curves shows that in the transverse direction (y), the resistance of the buildings without walls is significantly smaller than in the longitudinal one (x), yet this difference is strongly attenuated by the cooperation of the walls. In the initial segments, the curves for the buildings with walls are markedly above those of the buildings without walls; conversely, after these top curves reach their peaks, they descend abruptly and tend to converge with the bottom curves. As discussed previously, the short column effect possibly arising after the failure of the walls was not considered in this study. Therefore, the failure of the walls cannot damage the frame; simply, once the walls fail, the frame is "left alone" to resist the seismic forces. As the peaks appear to correspond to the collapse of the walls, this trend shows that the walls fail prior to the main structure; remarkably, points "●" (1st plastic hinge) are either coincident or slightly earlier than those peaks. The collapse of the walls and the subsequent failure of the columns bore, in most cases, the greatest impact on the overall system behavior. These global inferences apply for all the considered cases. Hence, observation of the Target Drifts and the other points shown in Table 6 lead us to the following conclusions applicable to Soil A and to design acceleration 0.08 g:

- Comparison between points "□" and "▷" indicates that the requirements of the design codes considered (assuming the aforementioned values of the response reduction factors) are often inadequate. For 3-story buildings without walls, the design codes tend to be slightly more demanding, whereas this situation clearly inverts for the cases with walls. For the 6-story buildings without walls the agreement between the seismic forces derived from push-over analyses and those prescribed by the codes is reasonable. For the 6-story buildings with low wall density the requirements of the design codes are clearly excessive, beyond the building capacity, particularly in the transverse direction (y). For the 6-story buildings with high wall density, the requirements of the design codes are commonly too low. These conclusions can be broadly generalized for design acceleration 0.11 g and the other soil types [7].
- Comparison between the positions of points "▷" and "●" shows that in the buildings with high wall density the Target Drift for LS is either earlier than the first plastic hinge or rather simultaneous, indicating a highly proper behavior. In buildings with low wall density or with no walls, however, this situation tends to attenuate or to reverse, particularly in the transverse direction (y) of the 6-story buildings without walls.
- Comparison between the positions of points "◇" and "∗" shows that in buildings with span-length 5 m the Target Drift for CP is slightly earlier than the first failure; this indicates a proper behavior. In 6-story buildings with 5.5 m span-length, points "◇" are not present; obviously, this means that such buildings collapse for inputs whose severity corresponds to CP.
- Comparison between the inception of yielding and the positions of points "□" shows that, taking into account the assumed response reduction factors (see Section 3), the buildings without walls do not fulfill the seismic design codes. The cooperation of the infill walls tends to improve this situation, although the design codes are still not fulfilled in all cases. Given that Figs. 7–12 correspond to the less demanding situation (e.g. stiff soil and low seismic design acceleration), in the other cases the degree of fulfillment is significantly lower.

Table 3 displays the capacity of the considered buildings in terms of the base shear coefficient, i.e. the maximum ordinates of the capacity curves displayed in Figs. 7–12.

In addition to the conclusions derived from Fig. 7 through Fig. 12, results from Table 3 show high variability, ranging in between 1% for the transverse direction (y) of building 6 – 5.5 – ■

Table 3
Maximum values of the base-shear coefficients (V/W) for the selected buildings.

Building	No walls		Low wall density		High wall density	
	Direction of the wide beams (x)	Transversal direction (y)	Direction of the wide beams (x)	Transversal direction (y)	Direction of the wide beams (x)	Transversal direction (y)
3 – 5 – ■	0.066	0.023	0.130	0.115	0.381	0.350
3 – 5.5 – ■	0.0595	0.021	0.128	0.108	0.425	0.415
6 – 5 – ■	0.028	0.012	0.060	0.047	0.145	0.140
6 – 5.5 – ■	0.025	0.010	0.058	0.045	0.145	0.140
6 – 5 – ■	0.033	0.013	0.065	0.053	0.178	0.165
6 – 5.5 – ■	0.035	0.015	0.073	0.0595	0.185	0.175

Table 4
Displacement ductility (μ) for the selected buildings.

Building	No walls		Low wall density		High wall density	
	Dir. of the wide beams (x)	Transversal direction (y)	Dir. of the wide beams (x)	Transversal direction (y)	Dir. of the wide beams (x)	Transversal direction (y)
3 – 5 – ■	2.23	2.69	2.05	2.07	2.02	2.02
3 – 5.5 – ■	2.35	**2.75**	2.35	2.42	2.12	2.17
6 – 5 – ■	1.89	2.10	1.79	2.00	1.48	1.55
6 – 5.5 – ■	2.01	2.33	1.98	2.02	1.90	1.98
6 – 5 – ■	1.75	1.90	1.70	1.82	**1.25**	1.58
6 – 5.5 – ■	1.70	1.85	1.65	1.78	1.50	1.54

without walls and 42.5% for the direction of the wide beams (x) of building 3 – 5.5 – ■ with high wall density.

Table 4 displays the displacement ductility, i.e. the ratio between the displacement corresponding to the maximum base shear and the yielding displacement (Figs. 7–12). The yielding point is defined, based on a bilinear approximation of the capacity curve, by the classical equal-area criterion [20].

Results from Table 4 show high variability, ranging 1.25 for the direction of the wide beams (x) of building 6 – 5 – ■ with high wall density to 2.75 for the transverse direction (y) of building 3 – 5.5 – ■ without walls. Since the ductility factors in Table 4 are roughly equal to the ratio between the yielding and collapse displacements, the important differences among them can be partly explained by the large number of phenomena involved in the yielding and the collapse of the building. Apart from this overall conclusion, Table 4 shows a fairly regular behavior, with expected results.

Fig. 13 shows the capacity curves of building 6 – 5.5 – ■ without walls for soil A and design ground acceleration 0.08 g. For each capacity curve, the damage intervals suggested by the research project RISK-UE [23] are indicated; "ND", "SD", "MD", "ED" and "HD" account for "No Damage", "Slight Damage", "Moderate Damage", "Extensive Damage" and "Heavy Damage" (collapse),

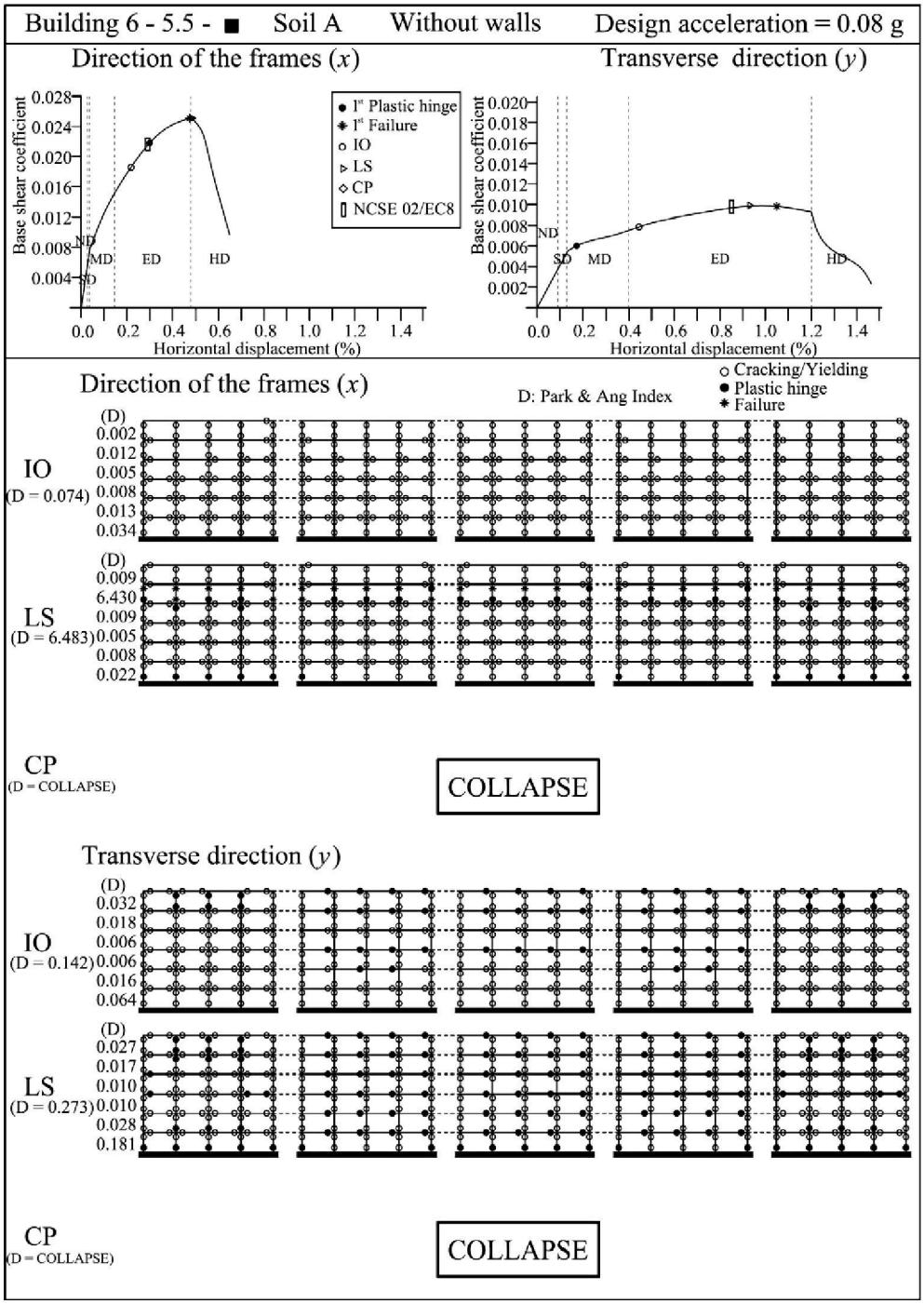

Fig. 13. Capacity curves, Target Drifts and sequence of formation of plastic hinges of building 6 – 5.5 – ■ without walls. Soil A and design acceleration 0.08 g.

Table 5
Damage level of the selected buildings. Target Drift IO ("Immediate Occupancy").

Building	Direction	Wall density	Design acceleration 0.08 g				Design acceleration 0.11 g			
			Soil A	Soil B	Soil C	Soil D	Soil A	Soil B	Soil C	Soil D
3 – 5 – ■	Wide beams (x)	None	MD	MD	ED	ED	MD	ED	ED	HD
		Low	MD	MD	ED	ED	MD	ED	ED	HD
		High	ND	SD	SD	MD	SD	SD	MD	ED
	Trans. (y)	None	MD	MD	ED	ED	MD	ED	ED	HD
		Low	MD	MD	ED	ED	MD	ED	ED	HD
		High	SD	SD	MD	MD	SD	MD	MD	MD
3 – 5.5 – ■	Wide beams (x)	None	MD	ED	ED	HD	MD	ED	HD	HD
		Low	MD	MD	ED	HD	MD	ED	ED	HD
		High	ND	SD	SD	MD	SD	MD	MD	ED
	Trans. (y)	None	MD	ED	ED	HD	MD	ED	ED	HD
		Low	MD	ED	ED	HD	MD	ED	ED	HD
		High	ND	SD	SD	MD	SD	MD	MD	ED
6 – 5 – ■	Wide beams (x)	None	MD	ED	HD	HD	ED	ED	HD	HD
		Low	SD	MD	ED	HD	MD	ED	HD	HD
		High	SD	MD	ED	HD	MD	ED	HD	HD
	Trans. (y)	None	ED	ED	HD	HD	ED	ED	HD	HD
		Low	MD	MD	ED	HD	MD	ED	HD	HD
		High	MD	MD	ED	HD	MD	ED	HD	HD
6 – 5.5 – ■	Wide beams (x)	None	ED	ED	HD	HD	ED	HD	HD	HD
		Low	MD	ED	HD	HD	ED	ED	HD	HD
		High	MD	ED	HD	HD	ED	ED	HD	HD
	Trans. (y)	None	ED	ED	HD	HD	ED	HD	HD	HD
		Low	MD	ED	HD	HD	ED	ED	HD	HD
		High	MD	ED	HD	HD	ED	ED	HD	HD
6 – 5 – ▌	Wide beams (x)	None	MD	ED	HD	HD	ED	ED	HD	HD
		Low	SD	MD	MD	HD	SD	ED	HD	HD
		High	SD	MD	MD	HD	SD	ED	HD	HD
	Trans. (y)	None	MD	ED	HD	HD	ED	ED	HD	HD
		Low	MD	MD	ED	HD	MD	ED	HD	HD
		High	SD	MD	ED	HD	SD	ED	HD	HD
6 – 5.5 – ▌	Wide beams (x)	None	ED	ED	HD	HD	ED	HD	HD	HD
		Low	MD	ED	HD	HD	ED	ED	HD	HD
		High	MD	ED	HD	HD	ED	ED	HD	HD
	Trans. (y)	None	ED	ED	HD	HD	ED	HD	HD	HD
		Low	MD	ED	HD	HD	MD	ED	HD	HD
		High	ND	ED	HD	HD	MD	ED	HD	HD

respectively. For a proper seismic behavior, Target Drifts for IO, LS and CP should correspond to SD, MD and ED, respectively [30]. The distribution of damage that corresponds to the Target Drifts for IO, LS and CP in each direction is indicated, in Fig. 13, in terms of the distribution and progression of the plastic hinges along the building frame and of the values of the Park and Ang damage index [27] in each floor and in the whole building. The damage levels indicated by the RISK-UE project were compared with those established by the Park and Ang index, giving satisfactory agreement. The assumed equivalences between the two indices are: ND ($D < 0.005$), SD ($0.005 < D < 0.03$), MD ($0.03 < D < 0.15$), ED ($0.15 < D < 1$) and HD ($D = 1$).

The sketches drawn in Fig. 13 show that in the direction of the wide beams (x), the earlier plastic hinges initiate and develop mainly in the columns, particularly in the lowest floors; and, the failures likewise commence in the columns. In the transverse direction (y), in the outer frames the hinges are first formed in the columns, while in the inner frames the hinges are first formed in the joists. This difference can be explained by the higher strength of the façade beams (Fig. 3c. These results can be broadly extrapolated to the other buildings without walls. The capacity curves displayed in Fig. 13 show that in both directions the behavior for Target Drifts IO and LS is not acceptable since it corresponds to excessive levels of damage. Aiming to generalize these conclusions, Tables 5–7 display the damage levels for the Target Drifts IO, LS and CP, respectively. To facilitate interpretation, the levels of damage are also indicated with a grey-scale code in these tables.

Results from Tables 5–7 show a regular behavior; i.e. the higher damage levels correspond to design ground acceleration 0.11 g, to Soil D, to buildings without walls, to 6-story buildings, and to

Table 6
Damage level of the selected buildings. Target Drift LS ("Life Safety").

Building	Direction	Wall density	Design acceleration 0.08 g				Design acceleration 0.11 g			
			Soil A	Soil B	Soil C	Soil D	Soil A	Soil B	Soil C	Soil D
3 – 5 – ■	Wide beams (*x*)	None	MD	ED	ED	HD	ED	HD	HD	HD
		Low	MD	ED	ED	HD	MD	ED	ED	HD
		High	SD	MD	MD	ED	MD	MD	ED	HD
	Trans. (*y*)	None	MD	ED	ED	HD	ED	ED	HD	HD
		Low	MD	ED	ED	HD	ED	ED	HD	HD
		High	MD	MD	MD	ED	MD	MD	ED	HD
3 – 5.5 – ■	Wide beams (*x*)	None	ED	ED	HD	HD	ED	HD	HD	HD
		Low	MD	ED	HD	HD	ED	HD	HD	HD
		High	MD	MD	ED	HD	MD	ED	HD	HD
	Trans. (*y*)	None	ED	HD	HD	HD	ED	HD	HD	HD
		Low	ED	HD	HD	HD	ED	HD	HD	HD
		High	MD	MD	ED	HD	MD	ED	HD	HD
6 – 5 – ■	Wide beams (*x*)	None	ED	HD	HD	HD	ED	HD	HD	HD
		Low	MD	HD	HD	HD	ED	HD	HD	HD
		High	MD	HD	HD	HD	ED	HD	HD	HD
	Trans. (*y*)	None	ED	HD	HD	HD	ED	HD	HD	HD
		Low	MD	HD	HD	HD	ED	HD	HD	HD
		High	MD	ED	HD	HD	ED	HD	HD	HD
6 – 5.5 – ■	Wide beams (*x*)	None	ED	HD	HD	HD	HD	HD	HD	HD
		Low	ED	HD	HD	HD	HD	HD	HD	HD
		High	ED	HD	HD	HD	HD	HD	HD	HD
	Trans. (*y*)	None	ED	HD	HD	HD	HD	HD	HD	HD
		Low	ED	HD	HD	HD	HD	HD	HD	HD
		High	ED	HD	HD	HD	HD	HD	HD	HD
6 – 5 – ▌	Wide beams (*x*)	None	ED	HD	HD	HD	ED	HD	HD	HD
		Low	MD	HD	HD	HD	ED	HD	HD	HD
		High	MD	ED	HD	HD	ED	HD	HD	HD
	Trans. (*y*)	None	ED	HD	HD	HD	ED	HD	HD	HD
		Low	ED	HD	HD	HD	ED	HD	HD	HD
		High	ED	ED	HD	HD	ED	HD	HD	HD
6 – 5.5 – ▌	Wide beams (*x*)	None	ED	HD	HD	HD	HD	HD	HD	HD
		Low	ED	HD	HD	HD	HD	HD	HD	HD
		High	ED	HD	HD	HD	HD	HD	HD	HD
	Trans. (*y*)	None	ED	HD	HD	HD	HD	HD	HD	HD
		Low	ED	HD	HD	HD	HD	HD	HD	HD
		High	ED	HD	HD	HD	HD	HD	HD	HD

Target Drift CP. Apart from these obvious inferences, results from Tables 5–7 give rise to the following conclusions:

- *Global assessment.* The damage is highly variable. For Target Drift LS (Table 6), it ranges notably between SD (building 3 – 5 – ■, *x* direction, high wall density, soil A) and HD. In most of the cases the damage is excessive for IO, LS and CP; in general, the performance tends to improve slightly from IO to CP.
- *Direction.* The damage levels in the transverse direction (*y*, see Figs. 2 and 3) are in most of the cases only slightly higher than in the direction of the wide-beam frames (*x*). This rather unexpected behavior might be explained, for the CP level, in light of the higher ductility in the transverse direction as compared to the ductility in the direction of the wide beams (see Table 4), which partially compensates the higher damage levels for IO and LS in the direction of the wide beams
- *Span-length.* In the cases without walls, the buildings with span-length 5.5 m exhibit higher damage levels. This trend is attenuated for low wall density, being inappreciable for high wall density.
- *Columns.* The comparison between buildings with square and rectangular columns does not show relevant differences. Remarkably, rectangular columns are more resistant and more ductile than the square ones, a difference generated by the lesser amount of reinforcement.

6. Dynamic analyses

A number of nonlinear dynamic analyses were carried out on the buildings of study (Table 1). The input accelerograms were taken from the European Strong-Motion data base [12]. Only registers whose response spectra roughly match the shape of the design

Table 7
Damage level of the selected buildings. Target Drift CP ("Collapse Prevention").

Building	Direction	Wall density	Design acceleration 0.08 g				Design acceleration 0.11 g			
			Soil A	Soil B	Soil C	Soil D	Soil A	Soil B	Soil C	Soil D
3 – 5 – ■	Wide beams (x)	None	ED	ED	HD	HD	ED	HD	HD	HD
		Low	ED	ED	HD	HD	ED	HD	HD	HD
		High	MD	MD	ED	HD	MD	HD	HD	HD
	Trans. (y)	None	ED	ED	HD	HD	ED	HD	HD	HD
		Low	ED	ED	HD	HD	ED	HD	HD	HD
		High	MD	MD	ED	HD	MD	HD	HD	HD
3 – 5.5 – ■	Wide beams (x)	None	ED	HD	HD	HD	HD	HD	HD	HD
		Low	ED	HD	HD	HD	ED	HD	HD	HD
		High	MD	ED	HD	HD	ED	HD	HD	HD
	Trans. (y)	None	ED	HD	HD	HD	ED	HD	HD	HD
		Low	ED	HD	HD	HD	ED	HD	HD	HD
		High	MD	ED	HD	HD	ED	HD	HD	HD
6 – 5 – ■	Wide beams (x)	None	ED	HD	HD	HD	HD	HD	HD	HD
		Low	ED	HD	HD	HD	HD	HD	HD	HD
		High	ED	HD	HD	HD	HD	HD	HD	HD
	Trans. (y)	None	ED	HD	HD	HD	HD	HD	HD	HD
		Low	ED	HD	HD	HD	HD	HD	HD	HD
		High	ED	HD	HD	HD	HD	HD	HD	HD
6 – 5.5 – ■	Wide beams (x)	None	HD	HD	HD	HD	HD	HD	HD	HD
		Low	HD	HD	HD	HD	HD	HD	HD	HD
		High	HD	HD	HD	HD	HD	HD	HD	HD
	Trans. (y)	None	HD	HD	HD	HD	HD	HD	HD	HD
		Low	HD	HD	HD	HD	HD	HD	HD	HD
		High	HD	HD	HD	HD	HD	HD	HD	HD
6 – 5 – ▌	Wide beams (x)	None	ED	HD	HD	HD	HD	HD	HD	HD
		Low	ED	HD	HD	HD	HD	HD	HD	HD
		High	ED	HD	HD	HD	HD	HD	HD	HD
	Trans. (y)	None	ED	HD	HD	HD	HD	HD	HD	HD
		Low	ED	HD	HD	HD	HD	HD	HD	HD
		High	ED	HD	HD	HD	HD	HD	HD	HD
6 – 5.5 – ▌	Wide beams (x)	None	HD	HD	HD	HD	HD	HD	HD	HD
		Low	HD	HD	HD	HD	HD	HD	HD	HD
		High	HD	HD	HD	HD	HD	HD	HD	HD
	Trans. (y)	None	HD	HD	HD	HD	HD	HD	HD	HD
		Low	HD	HD	HD	HD	HD	HD	HD	HD
		High	HD	HD	HD	HD	HD	HD	HD	HD

one [25] along the range of periods of interest, were selected. The accelerograms of reference were scaled to the design spectrum that corresponds to return period 500 years. The scaling consisted of multiplying the ordinates of the accelerogram by a single factor, whose value was determined so that the response spectrum of the scaled accelerogram was slightly above the design one as shown in Fig. 14b. Furthermore, the strongest input recently registered in Spain (Lorca earthquake, 11/05/2011) was also considered [17]. In the dynamic analyses, damping is described by a 5% Rayleigh model and the time step is 0.01 s in the European registers, and 0.005 s in the Lorca accelerograms. The nonlinear time integration was performed as in the push-over analyses (Section 5).

Fig. 14a shows the NS component of the Ambarli-Termik ground motion record of the Izmit earthquake (17/08/1999) [12]. In turn, Fig. 14b shows its response spectrum scaled to the design spectrum [25]. For comparison purposes, the design spectrum is also plotted. Fig. 15 displays the responses of building 3 – 5 – ■ to the scaled accelerogram.

Plots from Fig. 15 show that the building 3 – 5 – ■ without walls collapses. In the cases with walls, permanent displacements can be observed, particularly for low wall density; this indicates severe damage. The extension of these conclusions to the other considered buildings and to the other normalized inputs is discussed in the next section.

Fig. 16 shows the NS and EW components of the aforementioned Lorca accelerogram, while Fig. 17 shows the time-history displacement responses of the top floor of building 3 – 5 – ■ to such registers.

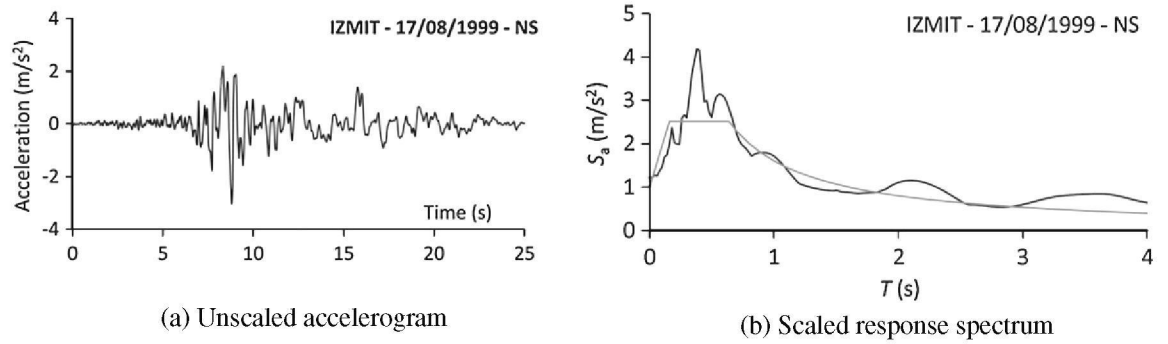

(a) Unscaled accelerogram (b) Scaled response spectrum

Fig. 14. NS component of the Ambarli-Termik ground motion record of the Izmit earthquake (17/08/1999).

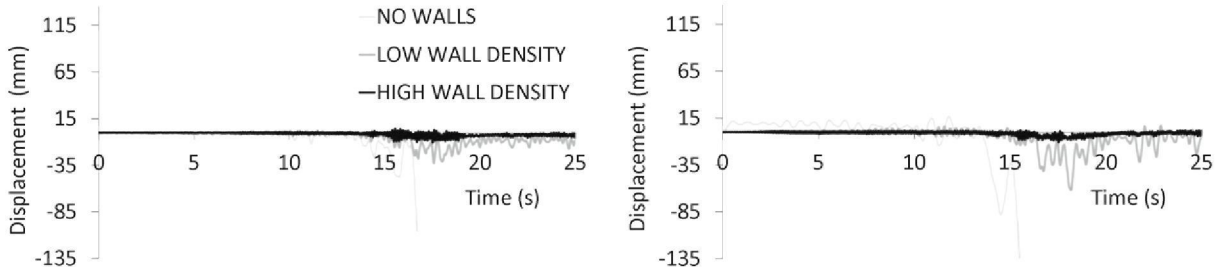

(a) Direction of the wide beams (x) (b) Transversal direction (y)

Fig. 15. Response of building 3 – 5 – ■ to the NS component of the Ambarli-Termik ground motion record of the Izmit earthquake (17/08/1999).

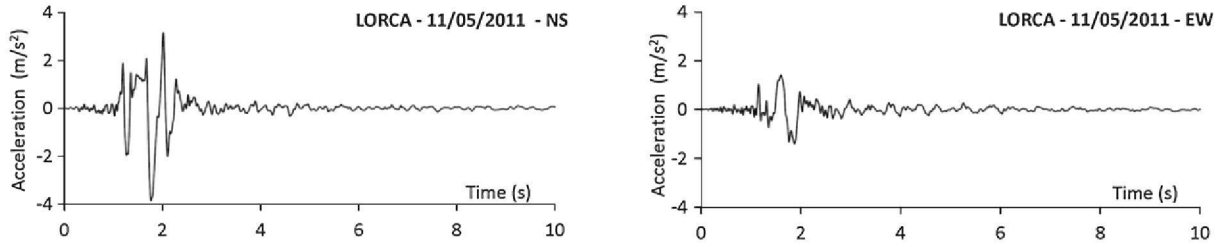

(a) North-South component (NS) (b) East-West component (EW)

Fig. 16. Accelerograms from the Lorca earthquake (11/05/2011).

Plots from Fig. 17 show that building 3 – 5 – ■ collapses, under the Lorca earthquake, in most of the cases. The only exceptions were the responses for high wall density in the direction of the less strong component (EW). These conclusions can be broadly generalized to the other 3-story buildings while the performance of the 6-story buildings is more deficient [7].

Table 8 presents response results on building 3 – 5 – ■ with high wall density. This building undergoes the simultaneous actuation of five pairs of scaled ground motion record components (NS and EW) selected from [12]. Results in Table 8 correspond to the percentages of the maximum displacement in each horizontal direction that are simultaneous with the maximum displacements in the orthogonal direction. The first/last two rows correspond to the NS/EW components of the input acting in the x direction of the building; in each row, the maximum displacements are considered in the highlighted directions.

Results from Table 8 show that in most of the analyzed cases, the usual criterion of combining the maximum value in one direction with 30% of the corresponding maximum in the orthogonal direction is sufficiently conservative. However, in one case, this percentage rises to 60%. The observation of analogous results corresponding to other buildings and other inputs provides similar conclusions [7].

7. Comparison between the code-type, push-over and dynamic analyses

Table 9 shows a comparison among the damage levels of buildings 3 – 5 – ■ and 6 – 5 – ■ corresponding to Target Drift LS obtained from three types of analyses: code-type analyses (Section 3), push-over analyses (Section 5) and dynamic analyses for the five scaled European registers considered in Table 8 (Section 6).

Results in Table 9 show that for building 3 – 5 – ■ the damage levels derived from dynamic analyses tend to be higher than those predicted by code-type and push-over analyses. This conclusion can be generalized to building 3 – 5.5 – ■ [7]. The discrepancy can be explained by the scaling criterion. Fig. 14b shows that the spectral ordinates of the scaled ground motion record exceed those of the design spectrum along several period ranges. For building 6 – 5 – ■, the damage levels derived from dynamic analyses tend to be similar to those predicted by code-type and push-over analyses, a conclusion that may be generalized to all the 6-story buildings [7].

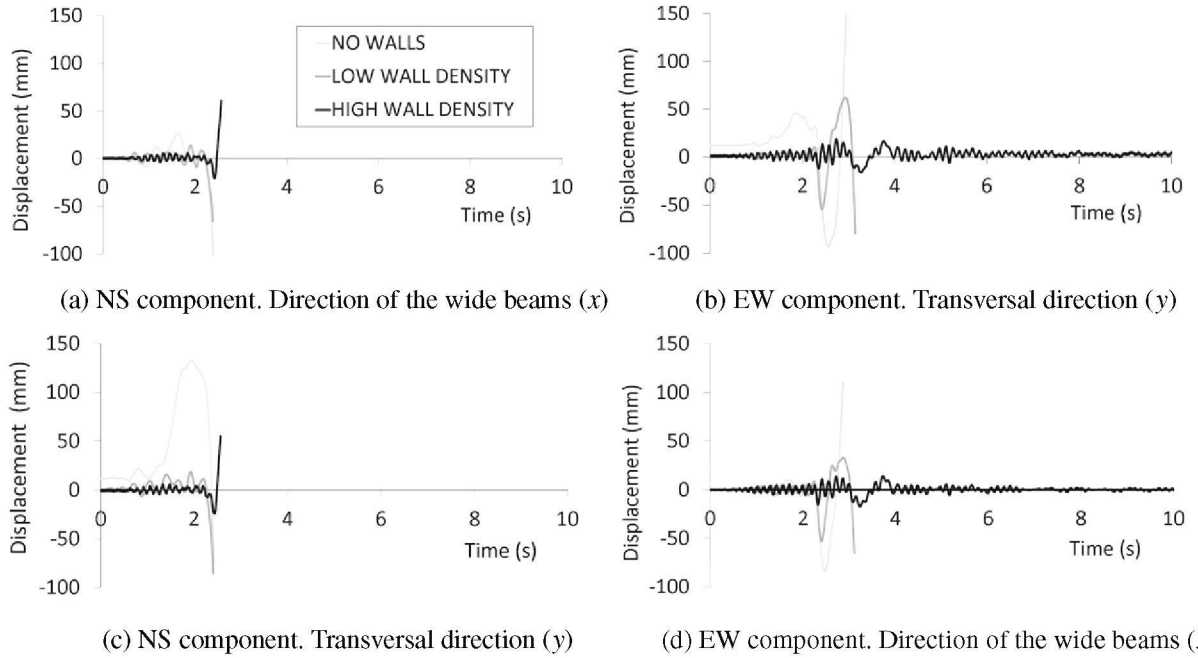

(a) NS component. Direction of the wide beams (x)

(b) EW component. Transversal direction (y)

(c) NS component. Transversal direction (y)

(d) EW component. Direction of the wide beams (x)

Fig. 17. Response of building 3 – 5 – ■ to the Lorca ground motion record (11/05/2011).

Table 8
Percentage of the maximum displacement in one direction that is simultaneous with the maximum displacement in the orthogonal direction. Building 3 – 5 – ■ with high wall density.

Input direction	Friuli (11/09/76)	Kalamata (13/09/86)	Izmit (17/08/99)	Izmit (17/08/99)	Duzce (12/11/99)
NS *x*/EW *y*	60	19	20	8	25
NS *x*/**EW *y***	28	17	1	1	48
NS *y*/EW *x*	53	19	9	0.4	15.5
NS *y*/**EW *x***	6	13	1.5	5.5	16

Table 9
Damage level of buildings 3 – 5 – ■ and 6 – 5 – ■ according to the dynamic, push-over and code-type analyses. Target Drift LS ("Life Safety").

Bldg.	Dir.	Wall density	Dynamic analyses: Friuli (11/09/76) (NS)	Kalamata (13/09/86) (NS)	Izmit (17/08/99) (NS)	Izmit (17/08/99) (EW)	Duzce (12/11/99) (EW)	Push -over	Code -type
3 – 5 – ■	Wide beams (x)	None	HD	HD	HD	HD	HD	ED	HD
		Low	HD	HD	SD	ND	HD	ED	ED
		High	MD	MD	ND	ND	MD	MD	ND
	Trans. (y)	None	HD	HD	HD	HD	HD	ED	HD
		Low	HD	HD	MD	SD	HD	ED	ED
		High	MD	MD	SD	ND	MD	MD	MD
6 – 5 – ■	Wide beams (x)	None	HD	HD	HD	HD	HD	HD	HD
		Low	HD	HD	HD	HD	HD	HD	HD
		High	HD	HD	ND	ND	HD	HD	ED
	Trans. (y)	None	HD	HD	HD	HD	HD	HD	HD
		Low	HD	HD	HD	HD	HD	HD	HD
		High	HD	HD	ND	ND	HD	HD	ED

8. Conclusions

This work presents a numerical study of the seismic vulnerability of RC buildings with one-way wide-beam slabs located in moderate seismicity regions of Spain; those edifices were designed without any seismic consideration. Two 3-story and four 6-story buildings were selected to represent the vast majority of the existing ones. Such edifices differ in their span-length (5 and 5.5 m) and in the cross-section of the columns (rectangular and square). The cooperation of the infill walls is accounted for; accordingly, for each building, three wall densities are considered: no walls, low density and high density. Vulnerability was investigated by code-type analyses, by push-over analyses and by nonlinear dynamic analyses. The torsional effects were not considered in the analyses.

The overall conclusion of this work is that the considered buildings show an inadequate seismic behavior in most of the

analyzed situations. The seismic performance, relative to the design requirements, tends to worsen as the return period of the design input decreases. Since these buildings are selected to be representative of the vast majority of buildings with wide beams that were constructed in Spain prior to 1994 without accounting for any seismic consideration, these conclusions can be generalized in this context.

Apart from these overall inferences, our study gives rise to the following particular conclusions:

- The cooperation of the infill masonry walls increases the seismic capacity in both directions significantly. However, the walls are less ductile than the main structure; thus, they fail prematurely.
- The first plastic hinges appear in the columns, except for the case of the inner frames in the transverse direction.
- The damage levels in the transverse direction are only slightly higher than those in the direction of the wide-beam frames.
- In the cases without walls, the buildings with longer span-length exhibit higher damage levels. This trend is attenuated for low wall density, being inappreciable for high wall density.
- The results for buildings with square and rectangular columns do not show relevant differences.
- Comparison between the LS performance points and the requirements of the considered design codes, indicates that such requirements are often inadequate; sometimes they are conservative and in other cases they are far from conservative.
- If the cooperation of the infill walls is not accounted for, the buildings do not fulfill the design codes. If such cooperation is considered, the design codes are fulfilled only in the less demanding situations.
- For the 3-story buildings the damage levels derived from dynamic analyses for inputs scaled to 500 year design spectra tend to be higher than those predicted by code-type and push-over (LS) analyses. For the 6-story buildings, all these damage levels tend to be similar.
- The considered buildings collapsed for the recent Lorca earthquake (Spain, 11/05/2011).
- In most of the analyzed cases, the customary criterion of combining the maximum displacement in one direction with 30% of the maximum displacement in the orthogonal direction is sufficiently conservative.

Achieving better seismic behavior for these structures involves important issues such as improving the detailing of the connections, avoiding the concentration of damage in given stories, preventing the failure of the plastic hinges at column ends, or increasing the overall energy dissipation capacity of the buildings by installing special devices (i.e. energy dissipators). Addressing these issues lies beyond the scope of the present study but is part of the work currently under progress by the authors.

Acknowledgements

This work has received financial support from the Spanish Government under projects CGL2008-00869/BTE, CGL2011-23621, BIA2008-00050 and BIA2011-26816 and from the European Union (Feder).

References

[1] ACI 318-08. Building code requirements for structural concrete and commentary. American Concrete Institute; 2008.
[2] Baber TT, Noori MN. Random vibration of degrading pinching systems. J Eng Mech 1985;111(8):1010–26.
[3] Benavent-Climent A. Seismic behavior of RC beam–column connections under dynamic loading. J Earthquake Eng 2007;11:493–511.
[4] Benavent-Climent A, Cahís X, Vico JM. Interior wide beam-column connections in existing RC frames subjected to lateral earthquake loading. Bull Earthq Eng 2010;8(2):401–20. http://dx.doi.org/10.1007/s10518-009-9144-3.
[5] Benavent-Climent A, Zahran R. An energy-based procedure for the assessment of seismic capacity of existing frames: application to RC wide beam systems in Spain. Soil Dyn Earthq Eng 2010;30(5):354–67.
[6] Bentz E, Collins MP. Response-2000, V. 1.0.5. Toronto, Ontario, Canada: Toronto University; 2000.
[7] Domínguez D. Evaluation of the earthquake-resistant capacity of wide-beam buildings located in low-to-moderate seismicity regions of Spain. Doctoral dissertation. Technical University of Catalonia; 2012 [in Spanish].
[8] EH-80. Directions for design and construction of plain or reinforced concrete structures. Ministerio de Obras Públicas y Urbanismo; 1980 [in Spanish].
[9] EN 1992. Eurocode 2. Design of concrete structures. European Committee for Standarization; 2004.
[10] EN 1996. Eurocode 6. Design of masonry structures. European Committee for Standarization; 2005.
[11] EN 1998. Eurocode 8. Design of structures for earthquake resistance. European Committee for Standarization; 2004.
[12] ESD. European strong-motion database. <http://www.isesd.hi.is/ESD_local/frameset.htm> [accessed 02.12].
[13] FEMA 356. Prestandard and commentary for the seismic rehabilitation of buildings. Federal Emergency Management Agency; 2000.
[14] Gentry RG, Wight JK. Wide beam-column connections under earthquake-type loading. Earthq Spectra 1994;10(4):675–703.
[15] Goldsworthy H, Abdouka K. Displacement-based assessment of non ductile exterior wide band beam-column connections. J Earthquake Eng 2012;16:61–82.
[16] Hatamoto H, Bessho S, Shibata T. Reinforced concrete wide-beam to column subassemblages subjected to lateral loads. ACI Publ 1991;SP-123:291–316.
[17] IGN. Series earthquake NE Lorca (Murcia) 11/05/2011. Instituto Geográfico Nacional. Public Works Ministry of Spain; 2011 [in Spanish].
[18] La Fave JM, Wight JK. Reinforced concrete exterior wide beam-column connections subjected to lateral earthquake loading. ACI Struct J 1999;96(4):577–85.
[19] La Fave JM, Wight JK. Reinforced concrete wide beam-column connections vs. conventional construction resistance to lateral earthquake loads. Earthq Spectra 2001;17(3):479–505.
[20] Mahin SA, Bertero VV. Problems in establishing and predicting ductility in aseismic design. In: Proceedings of the international symposium on earthquake structural engineering, St. Louis, Missouri; 1976. p. 613–28.
[21] Martínez JL, Martín JA, León J. Mechanical behavior of masonry. Monograph report on the structural analysis of historic constructions. Spain: Universidad Politécnica de Madrid; 2001 [in Spanish].
[22] Mehrabi AB, Shing PB, Schuller MP, Noland JL. Performance of masonry-infilled RC frames under in-plane lateral loads. Report CD/SR-94/6. University of Colorado at Boulder; 1994.
[23] Milutinovic ZV, Trendafiloski GS. Vulnerability of current buildings, work-package 4 of RISK_UE Project. European Commission, EVK4-CT-2000-00014; 2003.
[24] Mostafaei H, Kabeyasawa T. Effect of infill masonry walls on the seismic response of reinforced concrete buildings. Bulletin of the Earthquake Research Institute, vol. 79. University of Tokyo; 2004. pp. 133–156.
[25] NCSE 02. Norm for earthquake-resistant construction. Public Works Ministry of Spain; 2002 [in Spanish].
[26] Newmark NM. A method of computation for structural dynamics. J Eng Mech ASCE 1959;85(EM3):67–94.
[27] Park YJ, Ang AH. Mechanistic seismic damage model for reinforced concrete. J Struct Eng (ASCE) 1985;111(4):722–39.
[28] Paulay T, Priestley MJN. Seismic Design of Reinforced Concrete and Masonry Buildings. Wiley; 1992.
[29] Popov EP, Cohen E, Koso-Thomas K, Kasai K. Behavior of interior narrow and wide beams. ACI Struct J 1992;89(6):607–16.
[30] Pujades LG, Barbat AH, González-Drigo R, Avila J, Lagomarsino S. Seismic performance of a block of buildings representative of the typical construction in the Eixample district in Barcelona (Spain). Bull Earthq Eng 2012;10(1):331–49.
[31] Quintero-Febres CG, Wight JK. Experimental study of reinforced concrete interior wide beam-column connections subjected to lateral loading. ACI Struct J 2001;98(4):572–82.
[32] Reinhorn AM, Roh H, Sivaselvan M, Kunnath SK, Vallés RE, Madan A, et al. IDARC 2D Version 7.0. Program for the inelastic damage analysis of structures. MCEER technical report MCEER-09-006. State University of New York at Buffalo; 2009.
[33] Siah WL, Stehle JS, Mendis P, Goldsworthy H. Interior wide beam connections subjected to lateral earthquake loading. Eng Struct 2003;25:281–91.
[34] Stehle JS, Goldsworthy HM, Mendis P. Reinforced concrete interior wide band beam-column connections subjected to lateral earthquake loading. Am Concr Inst 2001;98(S26):270–9.
[35] Sugano S. Study on inelastic stiffness of reinforced concrete structures. Research reports of the annual meeting of the Architectural Institute of Japan Kanto Branch, vol. 3, Tokyo, Japan; 1968. p. 25–32.